Near-Infrared Surface Plasmon Resonance Measurements of Ultrathin Films. 2. Fourier Transform SPR Spectroscopy

ARTICLE *in* ANALYTICAL CHEMISTRY · SEPTEMBER 1999

Impact Factor: 5.64 · DOI: 10.1021/ac9905165

3 AUTHORS, INCLUDING:

Robert Corn
University of California, Irvine
193 PUBLICATIONS **10,574** CITATIONS

SEE PROFILE

Anal. Chem. **1999,** *71,* 3935−3940

Near-Infrared Surface Plasmon Resonance Measurements of Ultrathin Films. 2. Fourier Transform SPR Spectroscopy

Anthony G. Frutos,[†] Stephen C. Weibel,[‡] and Robert M. Corn[†]*

Department of Chemistry, University of Wisconsin—Madison, 1101 University Avenue, Madison, Wisconsin, 53706-1396, and GWC Instruments, 822 Oneida Place, Madison, Wisconsin, 53711

The application of surface plasmon resonance (SPR) measurements to the study of ultrathin organic films adsorbed onto gold surfaces utilizing near-infrared (NIR) excitation from a Fourier transform (FT) spectrometer is described. The FT-SPR experiment measures the NIR reflectivity spectrum from a prism/gold film/water assembly at a fixed angle of incidence approximately 1−2° greater than the critical angle. A strong reflectivity minimum is observed in the FT-SPR spectrum; this minimum can be shifted from 12 000 to 6000 cm^{-1} by tuning the angle of incidence. Upon adsorption of a thin biopolymer film from solution, a shift in the minimum is observed that can be correlated to a film thickness using Fresnel calculations. From experiments on the adsorption of electrostatically bound poly(lysine)/poly(glutamic acid) multilayers, an ∼60-cm^{-1} shift per 10-Å change in film thickness was measured. Frequency shifts of 2 cm^{-1} (corresponding to a thickness change of the polymer layer of ∼0.3 Å) can be easily measured from the FT-SPR spectra, demonstrating that this technique has sensitivity equivalent to or better than other visible SPR angle shift or wavelength shift measurements. Furthermore, the ability to perform FT-SPR measurements over a wide range of NIR wavelengths allows one to avoid any absorption bands that might otherwise interfere with the analysis.

Surface plasmon resonance (SPR) measurements are surface-sensitive techniques used to study thin films on Au and other noble metal surfaces.[1−6] These measurements can be performed in a number of different configurations including scanning angle (angle shift), wavelength shift, and imaging. In a typical scanning angle SPR measurement, the reflectivity of a p-polarized light beam (usually a HeNe laser) is measured as a function of incident angle from a prism/Au film assembly. At a certain incident angle, a minimum in the reflectivity is observed due to the creation of surface plasmons at the metal/dielectric interface. The position of this minimum—referred to as the SPR angle—is sensitive to the thickness and index of refraction of any adsorbed material on the metal surface. By monitoring shifts in the SPR angle, the amount of material adsorbed can be determined. This is the basis for the commercially available Biacore instrument which has been used to measure protein/protein, DNA/DNA, and DNA/enzyme interactions.[7,8] Though a red HeNe laser is usually used in such angle shift measurements, other wavelengths can be used. For example, Peterlinz and Georgiadis[9] used a two-color approach to determine both the thickness and index of refraction of a thin film. Recently, we have implemented near-IR wavelengths for both scanning angle SPR measurements and SPR imaging,[10] and others have also employed IR and near-IR wavelengths in SPR scanning angle techniques.[11−15]

An alternative method of performing an SPR experiment is to measure the reflectivity of a white light source from a prism/Au film assembly at a fixed angle of incidence. In this wavelength shift implementation, a minimum in reflectivity at a certain wavelength is observed, and as with the scanning angle measurement, the position of this minimum shifts upon the adsorption of material onto the metal surface. The utility of this technique using wavelengths in the visible region of the spectrum has been demonstrated by several researchers,[16−26] but to our knowledge,

[†] University of Wisconsin—Madison.
[‡] GWC Instruments.

(1) Welford, K. *Opt. Quantum Electron.* **1991**, *23*, 1−27.
(2) Burstein, E.; Chen, W. P.; Chen, Y. J.; Harstein, A. *J. Vac. Sci. Technol.* **1974**, *11*, 1004−1019.
(3) Frutos, A. G.; Corn, R. M. *Anal. Chem.* **1998**, *70*, 449A−455A.
(4) Hanken, D. G.; Jordan, C. E.; Frey, B. L.; Corn, R. M. *Electroanal. Chem.* **1998**, *20*, 141−225.
(5) Homola, J.; Yee, S. S.; Gauglitz, G. *Sens. Actuators B* **1999**, *54*, 3−15.
(6) Knoll, W. *MRS Bull.* **1991**, *16*, 29−39.
(7) Fagerstam, L. G.; O'Shannessy, D. J. In *Handbook of Affinity Chromatography*; Kline, T., Ed.; Marcel Dekker: New York, 1993; Vol. 63, pp 229−252.
(8) Szabo, A.; Stolz, L.; Granzow, R. *Curr. Opin. Struct. Biol.* **1995**, *5*, 699−705.
(9) Peterlinz, K. A.; Georgiadis, R. *Opt. Commun.* **1996**, *130*, 260−266.
(10) Nelson, B. P.; Frutos, A. G.; Brockman, J. M.; Corn, R. M. *Anal. Chem.* **1999**, *71*, 3928−3934.
(11) Yang, F.; Bradberry, G. W.; Sambles, J. R. *J. Mod. Opt.* **1990**, *37*, 993−1003.
(12) Yang, F.; Bradberry, G. W.; Jarvis, D. J.; Sambles, J. R. *J. Mod. Opt.* **1990**, *37*, 977−991.
(13) Brink, G.; Sigl, H.; Sackmann, E. *Sens. Actuators B* **1995**, *24−25*, 751−756.
(14) Bradberry, G. W.; Sambles, J. R. *Opt. Commun.* **1988**, *67*, 404−408.
(15) Melendez, J.; Carr, R.; Bartholomew, D.; Taneja, H.; Yee, S.; Jung, C.; Furlong, C. *Sens. Actuators B* **1997**, *38−39*, 375−379.
(16) Zhang, L. M.; Uttamchandani, D. *Electron. Lett.* **1988**, *24*, 1469−1470.
(17) Tubb, A. J. C.; Payne, F. P.; Millington, R. B.; Lowe, C. R. *Sens. Actuators B* **1997**, *41*, 71−79.
(18) Jory, M. J.; Vukusic, P. S.; Samples, J. R. *Sens. Actuators B* **1994**, *17*, 203−209.
(19) Jorgenson, R. C.; Yee, S. S. *Sens. Actuators B* **1993**, *12*, 213−220.
(20) Karlsen, S. R.; Johnston, K. S.; Yee, S. S.; Jung, C. C. *Sens. Actuators B* **1996**, *32*, 137−141.

10.1021/ac9905165 CCC: $18.00
Published on Web 08/18/1999

no wavelength shift measurements have been performed above ~900 nm.[27] In this paper we describe the use of a Fourier transform (FT) spectrometer to perform SPR wavelength shift measurements in the near-infrared (NIR) out to 2 μm on a gold surface. The use of an FT spectrometer allows for the rapid acquisition of SPR curves with high precision in wavelength and is especially suited to monitoring the in situ adsorption of analytes. This is demonstrated by a series of experiments in which the adsorption of alternating layers of poly(lysine) and poly(glutamic acid) (PG) onto a modified gold film is characterized in situ.

EXPERIMENTAL CONSIDERATIONS

Materials. The chemicals 11-mercaptoundecanoic acid (MUA) (Aldrich), absolute ethanol (Aaper), sodium dihydrogen phosphate monohydrate (Fluka), sodium hydrogen phosphate dihydrate (Fluka), (3-mercaptopropyl)trimethoxysilane (Aldrich), poly(L-lysine) hydrobromide (PL) (MW = 34 300, Sigma), and poly(L-glutamic acid) (PG) (MW = 95 000, Sigma) were all used as received. Millipore-filtered water was used for all aqueous solutions and rinsing.

Sample Preparation. Gold samples were prepared by vapor deposition of gold onto microscope slide covers (Fisher No. 2, 18 × 18 mm) or SF-10 glass slides (Schott Glass, 18 mm × 18 mm × 1 mm) that had been silanized with (3-mercaptopropyl)-trimethoxysilane in a manner similar to that reported by Goss et al.[28] Gold surfaces were modified with a monolayer of MUA by immersing the slide overnight in a 1 mM solution of the thiol in ethanol. The electrostatic adsorption of alternating layers of PL and PG was accomplished by exposing the surface to alternating 0.2 mg/mL solutions of the polypeptide in a pH 8, 100 mM phosphate buffer for 30 min. After each exposure step the surface was thoroughly rinsed by flushing the cell with ~5 mL of Millipore water.

Instrumental Apparatus. The experimental setup is depicted in Figure 1. The light beam from the external port of a Bruker Vector 22 equipped with a quartz beam splitter and quartz halogen light source was passed through a collimator and then polarized using a Polaroid NIR linear polarizing film (Edmund Scientific). The collimator consisted of a 2-in. FL lens (L1), a 1-mm pinhole, and a 6-in. FL lens (L2). Samples were brought into optical contact with an SF-10 equilateral prism (Coherent) using an $n = 1.730$ index matching fluid (Cargille) or a BK-7 right angle prism (Melles Griot) using ethylene glycol as an index matching fluid. (SF-10 and BK-7 prisms and sample substrates were used for in situ and ex situ experiments, respectively.) The prism/Au sample assembly was mounted onto a rotation stage, which allowed the angle of incidence (θ) to be changed. To measure the in situ adsorption of molecules onto the sample, a liquid flow cell with a volume of ~60 μL was attached to the back of the prism/Au sample assembly. The light reflected from this assembly was detected with either a Si or InGaAs photodiode. SPR reflectivity curves were generated using the spectrometer by first collecting a background scan with the polarizer set to s-polarization; a sample scan was then collected with the polarizer set to p-polarization. All FT-SPR spectra are the average of 32 scans collected at 8-cm^{-1} resolution. Shifts in the FT-SPR reflectivity minimums were measured to ±2 cm^{-1} by fitting a small region near the minimums to a quadratic.

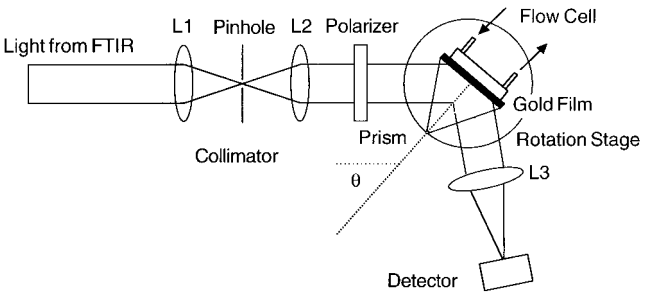

Figure 1. FT-SPR experimental setup. A prism/Au sample assembly is illuminated with collimated, polarized light from an FT spectrometer at a specific angle of incidence, θ, and the reflected light is detected with either a Si or InGaAs photodiode. The collimator consists of two lenses (L1 and L2) and a pinhole. The prism/Au sample assembly is mounted onto a rotation stage so that θ can be changed, and a liquid flow cell can be attached to the assembly for in situ adsorption measurements.

RESULTS AND DISCUSSION

Tuning the FT-SPR Wavelength Minimum. To demonstrate the spectral range available for FT-SPR experiments and to show how the SPR wavelength minimum can be tuned by changing the angle of incidence, FT-SPR reflectivity curves at a series of different angles were obtained from a 410-Å bare gold sample in contact with air (i.e., ex situ). Starting at an angle of incidence of ~42.90°, FT-SPR reflectivity curves were collected in angle increments of −0.08°. Figure 2a shows the results of this experiment with a Si photodiode detector. Notice that as the angle of incidence decreases, the SPR minimum shifts to lower energy. To obtain curves at wavenumbers smaller than ~10 000, the Si photodiode was replaced with an InGaAs detector; the data obtained using this detector (with an angle increment of −0.04°) are shown in Figure 2b. Notice that, in this ex situ configuration, the SPR reflectivity curves broaden as the angle of incidence decreases.

A similar experiment was performed on a 410-Å gold film in contact with water (i.e., in situ). In this experiment, FT-SPR reflectivity curves were collected in angle increments of −0.13° starting at an angle of incidence of 53.91°. Figure 3 shows the results of this experiment with both Si and InGaAs photodiode detectors. In contrast to the curves obtained in the ex situ experiment, the SPR curves in this in situ configuration sharpen with decreasing angle of incidence. The absorption overtone of water exerts a very small influence on the SPR reflectivity curves near ~7000 cm^{-1} as seen in the three rightmost curves in Figure 3b. However, the ability to tune the FT-SPR minimum allows such overtone absorption bands to be avoided.

The in situ configuration used to obtain the FT-SPR reflectivity curves shown in Figure 3 can be used to monitor the in situ

(21) Homola, J. *Sens. Actuators B* **1997**, *41*, 207−211.
(22) Aldinger, U.; Pfeifer, P.; Schwotzer, G.; Steinrucke, P. *Sens. Actuators B* **1998**, *51*, 298−304.
(23) Stemmler, I.; Brecht, A.; Gauglitz, B. *Sens. Actuators B* **1999**, *54*, 98−105.
(24) Hanning, A.; Roeraade, J.; Delrow, J. J.; Jorgenson, R. C. *Sens. Actuators B* **1999**, *54*, 25−36.
(25) Johnston, K. S.; Mar, M.; Yee, S. S. *Sens. Actuators B* **1999**, *54*, 57−65.
(26) Jory, M. J.; Bradberry, G. W.; Cann, P. S.; Sambles, J. R. *Meas. Sci. Technol.* **1995**, *6*, 1193−1200.
(27) One report does describe the ellipsometric detection of surface plasmons generated in the infrared for a thick quartz film on an aluminum substrate. However, no wavelength shift or thickness measurements were performed. See: Roeseler, A.; Goulz, M.; Trutschel, U.; Abraham, M. *Opt. Commun.* **1989**, *70*, 8−11.
(28) Goss, C. A.; Charych, D. H.; Majda, M. *Anal. Chem.* **1991**, *63*, 85−88.

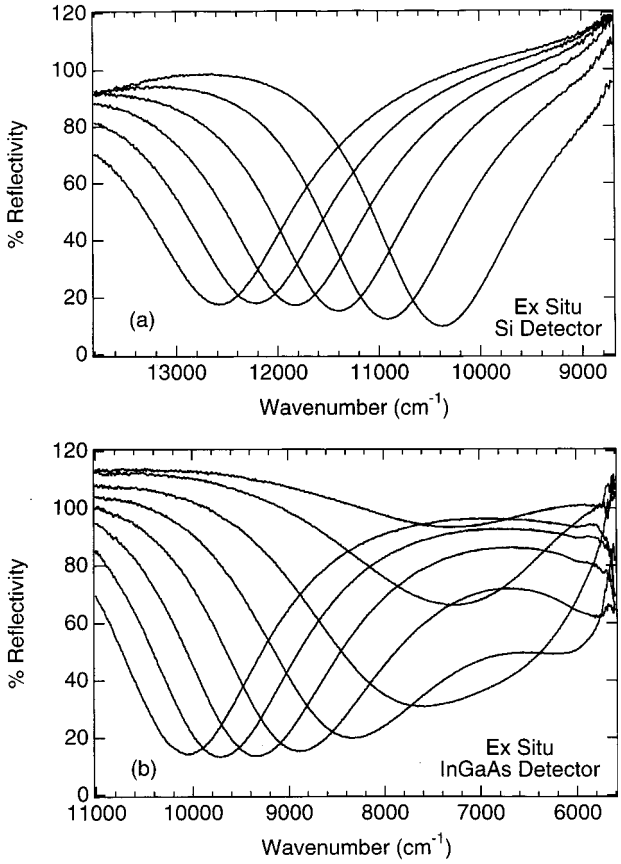

Figure 2. Ex situ FT-SPR reflectivity curves obtained at a variety of incident angles. Starting at an incident angle of 42.90°, the reflectivity curves of a 410-Å gold film in contact with air (ex situ) were collected in angle increments of (a) −0.08 and (b) −0.04°. To collect FT-SPR reflectivity curves at energies of <∼10 000 cm^{-1}, the Si detector was replaced with an InGaAs detector. As the angle of incidence decreases, the SPR minimum shifts to lower energy and the reflectivity curves broaden as predicted by the theoretical plots shown in Figure 5a. Each spectrum is the average of 32 scans collected at 8 cm^{-1} resolution.

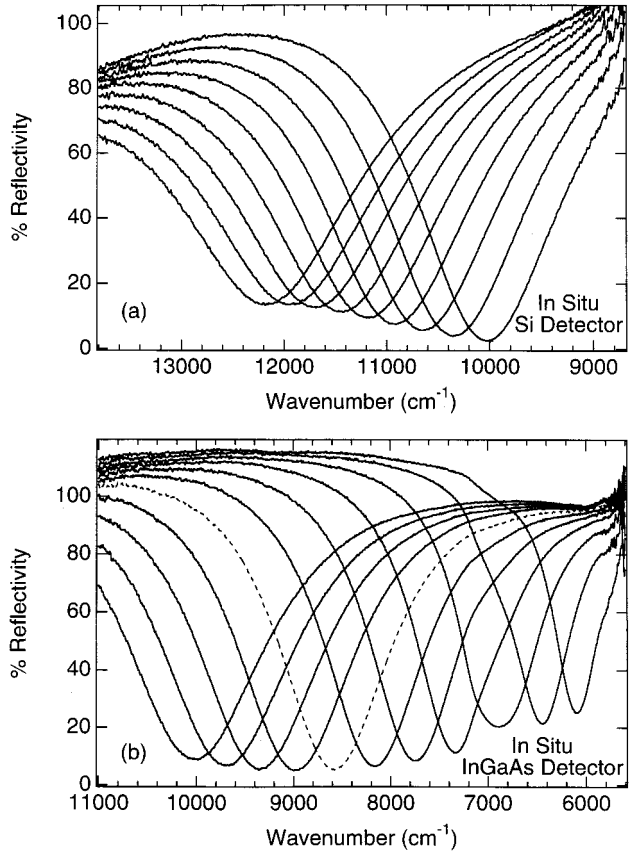

Figure 3. In situ FT-SPR reflectivity curves obtained at a variety of incident angles. The reflectivity curves of a 410-Å gold film in contact with water (in situ) were collected in angle increments of −0.13° starting at an angle of incidence of 53.91°. Notice that as the angle of incidence decreases, the reflectivity curves sharpen as predicted by the theoretical plots shown in Figure 5b. The dashed curve corresponds to the approximate fixed angle used in the in situ adsorption experiments shown in Figure 4. Each spectrum is the average of 32 scans collected at 8 cm^{-1} resolution.

adsorption of molecules onto a chemically modified gold surface. Such adsorption experiments could be performed over a wide spectral range, from ∼1 2 000 to ∼6000 cm^{-1}, depending upon the angle of incidence, thus allowing absorption bands to be avoided that might otherwise interfere with the analysis. The fixed angle used to monitor the in situ adsorption of polypeptides onto a chemically modified gold film described in the next section corresponds to the dashed reflectivity curve in Figure 3b. This angle was chosen because the SPR curve at this angle is relatively narrow and lies in the middle of the detection range of the InGaAs photodiode.

Multilayer Adsorption Experiments. To demonstrate that FT-SPR can be used to monitor and quantify the adsorption of analytes from solution onto modified gold surfaces, a series of sequential adsorption experiments was performed. Recently it has been shown that multilayer films can be formed in a layer-by-layer (LbL) electrostatic assembly by exposing charged surfaces to solutions containing oppositely charged polymers.[29−33] For example, by starting with a negatively charged carboxylate-terminated surface, multilayer films can be formed by alternating layers of polycationic PL and polyanionic PG. We have characterized this PL/PG multilayer assembly using FT-SPR measurements to demonstrate the application of this method to the in situ characterization of multilayer films. In these experiments, an InGaAs detector was used and the angle of incidence was fixed at 52.33°. A sample with a 410-Å gold film was modified with a monolayer of the alkanethiol MUA and then assembled in an in situ SPR flow cell in contact with water. The SPR reflectivity spectrum obtained from this surface is shown as the dotted curve in Figure 4. A layer of PL was then adsorbed from solution onto this MUA-modified gold surface, resulting in a shift of the SPR reflectivity minimum of −126.8 cm^{-1} as shown by the first solid curve in Figure 4. This Au/MUA/PL surface was subsequently modified by the adsorption of a layer of PG, which resulted in an additional shift of −63.2 cm^{-1} (first dashed curve). This series of PL/PG adsorption steps was repeated seven times (for clarity,

(29) Decher, G.; Hong, J. D. *Ber. Bunsen-Ges. Phys. Chem.* **1991**, *95*, 1430−1434.
(30) Decher, G. *Science* **1997**, *277*, 1232−1237.
(31) Decher, G.; Eckle, M.; Schmitt, J.; Struth, B. *Curr. Opin. Colloid Interface Sci.* **1998**, *3*, 32−39.
(32) Knoll, W. *Curr. Opin. Colloid Interface Sci.* **1996**, *1*, 137−143.
(33) Advincula, R.; Aust, E.; Meyer, W.; Knoll, W. *Langmuir* **1996**, *12*, 3536−3540.

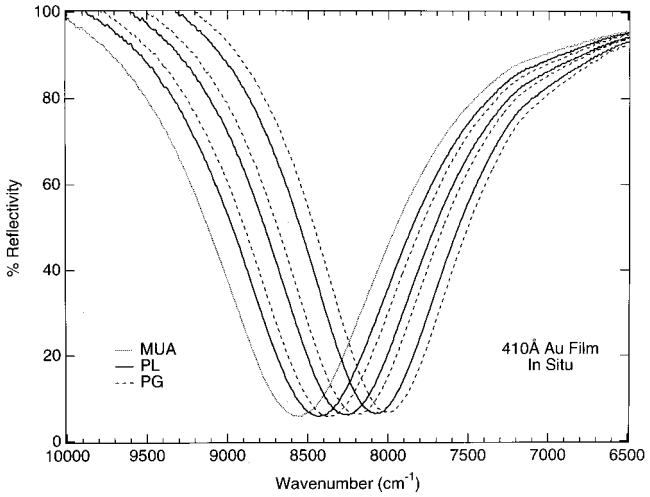

Figure 4. FT-SPR spectra for in situ adsorption measurements. These curves were taken at a fixed angle of 52.33° during the sequential adsorption of alternating layers of positively charged PL and negatively charged PG onto a MUA-modified gold film. The shift in minimum upon adsorption of each layer can be correlated to a change in thickness using Fresnel calculations. Each spectrum is the average of 32 scans collected at 8 cm^{-1} resolution.

Table 1. Wavenumber Minimums and Calculated Layer Thickness for in Situ Adsorption Experiments

surface	W_{min} (cm^{-1})	ΔW_{min} (cm^{-1})	Δd calc (Å)[a]
MUA	8557.1		
PL1	8430.3	126.8	17.5
PG1	8367.1	63.2	9.0
PL2	8260.1	107.0	15.5
PG2	8190.7	69.4	10.5
PL3	8075.0	115.7	17.5
PG3	8002.6	72.4	11.5
PL4	7882.1	120.5	19.0
PG4	7808.4	73.7	12.0
PL5	7681.5	126.9	22.0
PG5	7602.5	79.0	13.5
PL6	7473.3	129.2	23.0
PG6	7390.4	82.9	15.5
PL7	7263.1	127.3	24.0
PG7	7185.6	77.5	15.5

[a] An index of refraction of 1.52 was assumed for the polypeptide layers.

only the first set of three adsorption steps are shown in the figure). Table 1 lists the frequency minimum and corresponding shift in wavenumber for each layer. The shift in wavenumber minimum for each adsorption step was used in conjunction with Fresnel calculations to determine the thickness of each adsorbed layer as described in the following sections.

Theoretical Contour Plots. N-Phase Fresnel calculations can be utilized to model SPR reflectivity curves for different combinations of wavelength and angle. For example, Figure 5 shows theoretical plots of wavelength vs angle of incidence for a 410-Å gold film in both ex situ and in situ configurations. Each curve or contour represents a region of constant reflectivity from 1 to 50%. The dashed line in each plot represents the wavelength dependence of the critical angle for the BK-7/air interface or the SF-10/water interface. These contours were calculated using three-phase Fresnel calculations[34] and take into account the dispersion of the prism, gold, and water. (The dispersion equations for the

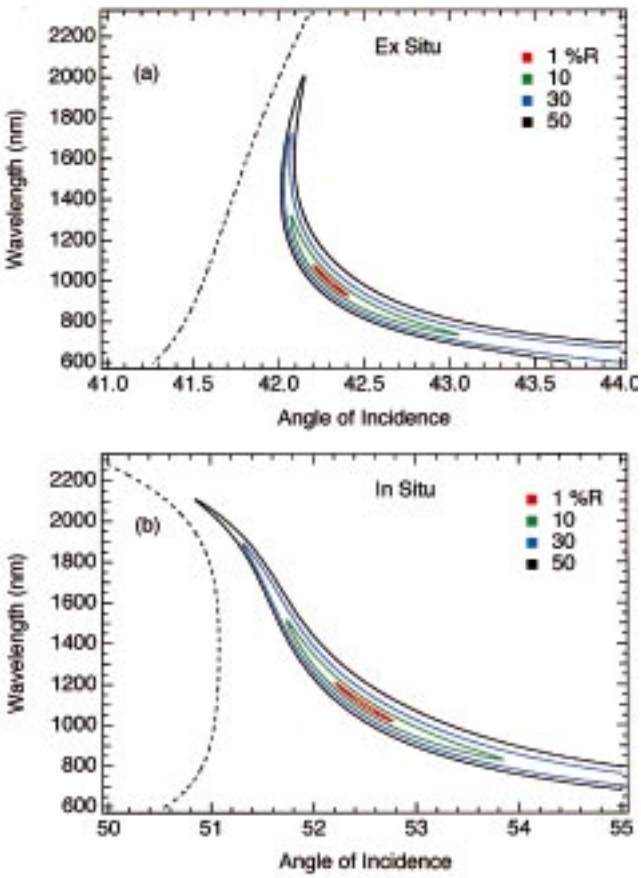

Figure 5. SPR reflectivity contour plots. These contours were generated from three-phase Fresnel calculations and show regions of constant reflectivity from 1 to 50% as a function of wavelength and angle of incidence. The contours in (a) are for an ex situ configuration (BK-7/Au/ air) and the contours in (b) are for an in situ configuration (SF-10/Au/water). The dashed line shows the wavelength dependence of the critical angle.

BK-7 and SF-10 prisms were obtained from Schott glass and the dispersion equation for water was obtained from eq 1 in ref 35; a dispersion equation for gold was generated by fitting the real and imaginary parts of the index of refraction data obtained by Johnson and Christy[36] to a polynomial.) Theoretical scanning angle SPR curves (reflectivity vs angle) can be generated from these contour plots by taking slices parallel to the *x*-axis at a fixed wavelength. As shown in Figure 5b, for a 410-Å gold film in contact with air, an SPR curve with a minimum reflectivity of 1% could be obtained by using a fixed wavelength between ~900 and 1100 nm. The use of NIR wavelengths for scanning angle SPR measurements is discussed in more detail elsewhere.[10]

In this paper, the experimental FT-SPR curves shown in Figures 2 and 3 correspond to slices through the contours parallel to the *y*-axis. In Figure 5b, the theoretical contour plot predicts that, for a 410-Å gold thin film in contact with water, an SPR minimum with a 1% reflectivity would occur between 1000 and 1200 nm (10000−8300 cm^{-1}) in qualitative agreement with the

(34) Hansen, W. N. *J. Opt. Soc. Am.* **1968**, *58*, 380−390. (These calculation programs are available on our web site at http://corninfo.chem.wisc.edu/calculations.html.)
(35) Thormahlen, I.; Straub, J.; Grigull, U. *J. Phys. Chem. Ref. Data* **1985**, *14*, 933−945.
(36) Johnson, P. B.; Christy, R. W. *Phys. Rev. B* **1972**, *6*, 4370−4379.

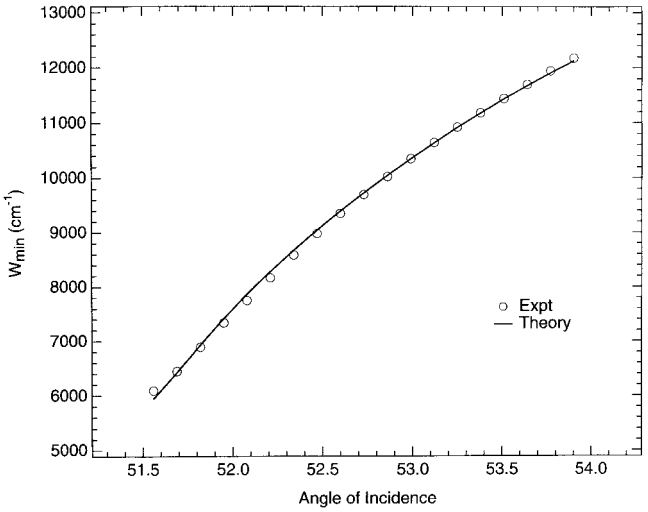

Figure 6. FT-SPR minimum as a function of incident angle for an SF-10/Au/water assembly. The open circles are the experimental minimums from Figure 3 and the solid line represents a three-phase (SF-10/Au/water) Fresnel calculation which takes into account the dispersion of all three phases. The optical constants of gold were derived from data taken by Johnson and Christy.[36]

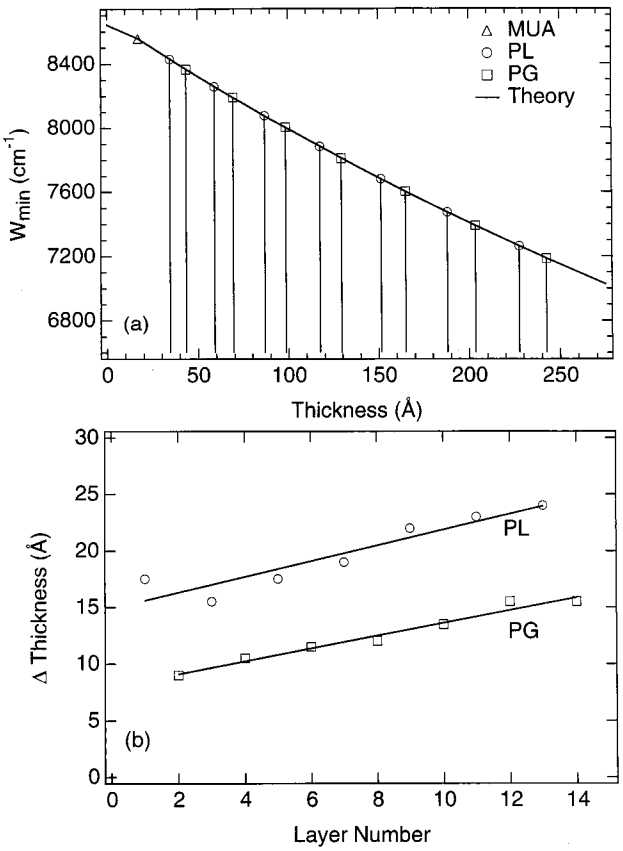

Figure 7. Analysis of in situ adsorption experiments. (a) Shift in frequency of the SPR minimum upon the sequential adsorption of PL and PG layers. The observed shift in the minimum is converted to a change in thickness by using a five-phase (SF-10/Au/MUA/polypeptide/water) Fresnel calculation indicated by the black line. Note that the shift in the minimum is not equivalent for the PL and PG. This is more clearly seen in (b) in which the change in thickness of each layer is plotted vs layer number. Note that each PL layer is thicker than each PG, and the thickness of each of these layers increases with layer number.

experimental curves shown in Figure 3. The change in the FT-SPR reflectivity curves (reflectivity vs wavelength) with angle of incidence is different for samples in contact with air (ex situ) and water (in situ). For example, notice that as the vertical cuts through the contours move toward smaller angles of incidence, the SPR curves become narrower for the in situ configuration but broaden ex situ. Specifically, the width of the 50% contour line in the ex situ configuration shown in Figure 5a broadens from 150 nm at an angle of incidence of 42.6° to 366 nm at 42.1°; conversely, the width of the 50% contour line in the in situ configuration shown in Figure 5b narrows from 190 nm at 52.6° to 171 nm at 51.6°. This difference was also observed experimentally as seen in Figures 2b and 3b. Also notice that for the ex situ configuration the BK-7/air critical angle moves to progressively larger angles with increasing wavelength (see Figure 5a). This increase has the effect that the SPR reflectivity curves (reflectivity vs wavelength) broaden at smaller angles of incidence, and at small enough angles, SPR curves containing two minimums are obtained; one such curve can be seen in Figure 2b. In contrast, for the in situ configuration, the SF-10/water critical angle shifts to smaller angles at longer wavelengths so that the curves sharpen with smaller angles of incidence.

Analysis of SPR Wavelength Tuning Experiments. Complex Fresnel calculations were also used to model the observed shift in SPR wavenumber minimum with incident angle. Figure 6 shows a plot of the observed SPR minimum as a function of angle of incidence for the series of curves in Figure 3. The open circles are the experimentally observed shifts and the solid line is a three-phase (SF-10/Au/water) Fresnel calculation which takes into account the dispersion of the prism, gold, and water. The dispersion equation for the gold was obtained by a polynomial fit to the optical constants of gold measured by Johnson and Christy,[36] with the imaginary part of the refractive index obtained from the fit being reduced by 2.2%. It has been noted that the optical constants of a gold thin film can vary depending upon sample preparation,[37] and hence a 2.2% modification is a very minor adjustment. The good agreement between theory and experimental data indicates that the optical constants for the prism, gold, and water used in the Fresnel calculations are accurate. A knowledge of these optical constants is necessary in order to make accurate thickness measurements of material adsorbed from solution onto the gold surface.

Analysis of Multilayer Adsorption Experiments. The shift in wavenumber minimum upon adsorption of each polypeptide (PL/PG) layer shown in Figure 4 was correlated with a change in thickness by using a five-phase (SF-10/Au/MUA/polypeptide/water) Fresnel calculation. In this calculation, the optical constants for the prism, gold, and water were those used to fit the data in Figure 6, and the indexes of refraction of the MUA and polypeptide monolayers were assumed to be 1.45[38] and 1.52,[39,40] respectively. The theoretical wavenumber minimum vs monolayer thickness

(37) Aspenes, D. E.; Kinsbron, E.; Bacon, D. D. *Phys. Rev. B* **1980**, *21*, 3290−3299.
(38) Bain, C. D.; Troughton, E. B.; Tao, Y. T.; Evall, J.; Whitesides, G. M.; Nuzzo, R. G. *J. Am. Chem. Soc.* **1989**, *111*, 321−335.
(39) Luckham, P. F.; Klein, J. *J. Chem. Soc., Faraday Trans. 1* **1984**, *80*, 865−878.
(40) Jordan, C. E.; Frey, B. L.; Kornguth, S.; Corn, R. M. *Langmuir* **1994**, *10*, 3642−3648.

is plotted in Figure 7a as the solid line. Also shown in the figure as the circles and squares are the experimentally observed minimums after each layer of PL and PG, respectively. The shift in minimum of -126.8 cm^{-1} upon adsorption of the first PL layer (PL1) corresponds to a change in thickness of 17.5 Å, and the additional shift of -63.2 cm^{-1} upon the subsequent adsorption of the first PG layer (PG1) corresponds to a thickness change of 9 Å. The change in thickness for each PL and PG layer vs layer number is shown in Figure 7b. Notice that each PL layer is thicker than the corresponding PG layer, and the thickness of both layers increases with layer number. These observations are consistent with FTIR and SPR angle shift measurements performed on similar samples. A shift in wavenumber/thickness can be estimated from the slope of the best-fit line through the points in Figure 7a and is $\sim$60 cm^{-1}/10 Å. Using a quadratic fit to a small region near the minimum of the FT-SPR reflectivity curves obtained at a nominal resolution of 8 cm^{-1}, wavenumber minimums can be measured to $\pm$2 cm^{-1}. (Similar results can be obtained from higher nominal resolution scans.) This corresponds to a detection limit of $\sim$0.3 Å, which compares favorably to the detection limit of conventional SPR angle shift and wavelength shift measurements of 0.1$-$3 Å.[21,22,41,42]

One source of error in making absolute thickness measurements using SPR techniques is uncertainty in knowing the refractive index of the adsorbed monolayer. This error is larger for measurements performed in situ than ex situ because the index of refraction of the adsorbed layer is closer to that of water ($n = 1.33$) than of air ($n = 1$). In estimating film thickness using SPR measurements, the refractive index of the monolayer is usually assumed to be the same as the bulk index of refraction. For the measurements in this paper, we have assumed the index of refraction for the monolayers to be the same as the bulk values and constant over the wavelength range. However, Peterlinz and Georgiadis[9] have demonstrated that both the thickness and index of refraction of thin films can be determined using scanning angle SPR measurements at two different wavelengths. In principle, by making measurements at multiple angles, the FT-SPR technique can be utilized in an analogous manner to determine both the thickness and index of refraction of a thin film.[43]

SUMMARY AND CONCLUSIONS

A new implementation of SPR measurements has been described which utilizes NIR wavelengths and an FT spectrometer to monitor and characterize the in situ adsorption of molecules onto modified gold films. These NIR FT-SPR measurements can be performed over a wide wavelength range, from $\sim$12 000 to $\sim$6000 cm^{-1}, by selecting an appropriate angle of incidence, with a sensitivity comparable to other SPR measurements. The advantages of the FT-SPR implementation include (i) the ability to rapidly acquire sets of SPR reflectivity curves during the course of an adsorption experiment and (ii) the ability to determine the absolute position of the wavenumber minimum with high accuracy. Furthermore, the ability to perform FT-SPR measurements over a wide range of NIR wavelengths allows one to avoid absorption bands that might otherwise interfere with the measurement. Future experiments will pursue the use of multiple angles to determine both the thickness and index of refraction of adsorbed layers.

ACKNOWLEDGMENT

The authors gratefully acknowledge the support of the National Science Foundation in these studies (Grants CHE-9626607, CCR-9613799, and CCR-9628814).

Received for review May 13, 1999. Accepted July 2, 1999.

AC9905165

(41) Jung, L. S.; Campbell, C. T.; Chinowsky, T. M.; Mar, M. N.; Yee, S. S. *Langmuir* **1998**, *14*, 5636−5648.
(42) Yeatman, E. M. *Biosens. Bioelectron.* **1996**, *11*, 635−649.
(43) Johnston, K. S.; Karlsen, S. R.; Jung, C. C.; Yee, S. S. *Mater. Chem. Phys.* **1995**, *42*, 242−246.